Simulation Model of High-Temperature Steam Oxidation in Cr-Coated Zirconium Cladding

Louis Metay Peault[1,2], Mauricio Exequiel Cazado[1], Fabrizio Gabrielli[1]

[1]Karlsruhe Institute of Technology (KIT), Institute for Neutron Physics and Reactor Technology (INR), RPD Group, Germany
[2]Grenoble INP – ENSE[3], France

1. Motivation and objective

- **The challenge:** under LOCA conditions, Zr oxidises rapidly generating significant heat and hydrogen: $Zr + 2\,H_2O \longrightarrow ZrO_2 + 2\,H_2$.
- **The ATF approach:** Cr-coated Zr cladding is an Advanced Technology Fuel (ATF) concept designed to delay high-temperature oxidation. The Cr coating ($4\,\mu m$ to $30\,\mu m$) forms a protective Cr_2O_3 scale that strongly reduced the oxidation rate.
- **The limitation:** protection is temporary. Zr–Cr interdiffusion forms $ZrCr_2$, contributing to Cr consumption, while outward Zr diffusion along Cr grain boundaries forms ZrO_2 pathways. TThese processes progressively degrade the protective capability of the coating, even while metallic Cr is still present.
- **Objective:** develop a mechanistic 1D solver that couples diffusion and thermodynamic phase equilibria to model oxidation and progressive loss of coating protection.

2. Numerical framework

The model is based on **species diffusion** described by an advection-diffusion formulation in the laboratory frame, which accounts for diffusion relative to the crystal lattice and the lattice motion induced by local volume changes:

$$\frac{\partial C_k}{\partial t} + \frac{1}{r}\frac{\partial}{\partial r}\left(r\, v\, C_k\right) = \frac{1}{r}\frac{\partial}{\partial r}\left(r\, D_k(T)\, \frac{\partial C_k}{\partial r}\right)$$

This is discretised in 1D cylindrical geometry using **Finite-Volume Method** with implicit time integration, upwind advection, and central differencing of diffusive fluxes.

Arbitrary Lagrangian–Eulerian (ALE) mesh: The mesh nodes move at a fraction of the interface velocity depending on their distance to the boundary. The material also moves due to volume changes resulting in a relative velocity: ($v_{\mathrm{rel}} = v_{\mathrm{mat}} - v_{\mathrm{mesh}}$).

3. Separate-Effects Modeling Method

Mechanisms implemented and validated as **stand alone models** before coupling.

- **Zr baseline** — O diffusion controlls ZrO_2 and α-Zr(O).
- **Chromia** — Cr diffuses to form Cr_2O_3.
- **$ZrCr_2$** — Controlled by the diffusion of Cr through Zr.
- **Coupled** — non-homogeneous phases: intergranular ZrO_2 path and Cr_2O_3 reduction.

Figure 1: Assembled domain (5 phases, 5 boundaries).

4. Zirconium baseline validation

The model was validated against isothermal oxidation experiments conducted at multiple temperatures. **Figure 2** shows a very good agreement between the predicted and experimental oxygen concentration profiles at 1200 °C versus depth. Interface jumps and diffusion tails are accurately captured across two orders of magnitude in time. Additionally, the Zr/ZrO_2 Pilling–Bedworth ratio (PBR) was recovered within 1.2% deviation, confirming volumetric consistency.

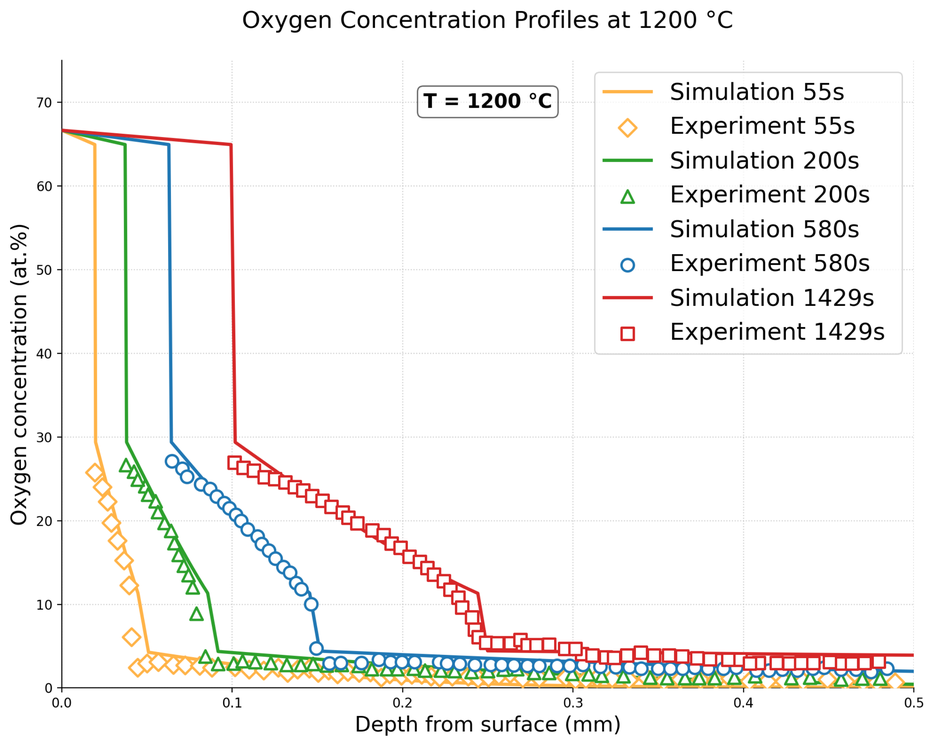

Figure 2: Oxygen concentration profiles validated against experimental data at $1200\,^{\circ}C$ [2].

5. Cr_2O_3 and $ZrCr_2$ validation

The kinetics of chromia (**Figure 3**) and intermetallic (**Figure 4**) layers were validated against experimental data for different isothermal conditions. Despite some deviations, the simulations results show good agreement with the measurements. Furthermore, the Cr_2O_3 PBR obtained matches the theoretical values within $0.45\,\%$.

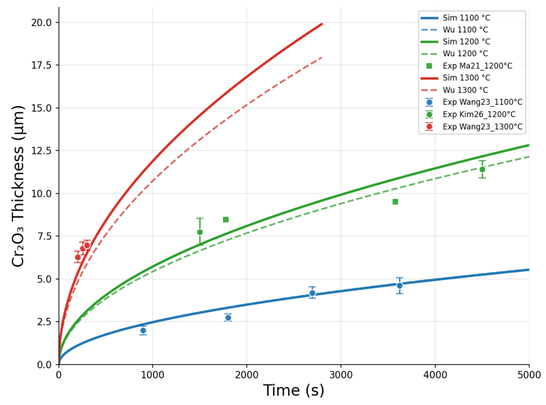

Figure 3: Chromia thickness vs. experimental data [1,4] under isothermal steam conditions ($1100\,^{\circ}C$ to $1300\,^{\circ}C$).

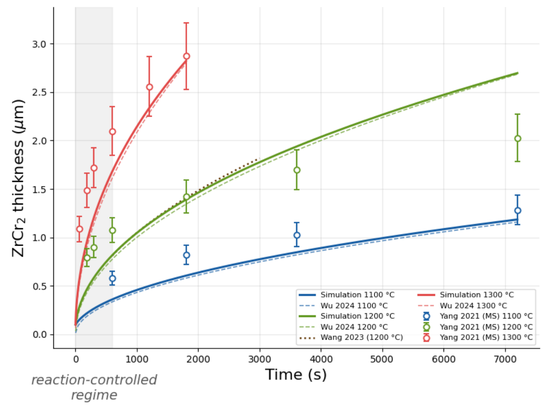

Figure 4: Comparison of simulated $ZrCr_2$ thickness with experimental data measured in Ar environment [5].

6. The coupled model: Two-Stage Degradation Mechanisms Incorporation

- t_1 **— ZrO_2 network "percolation":** Zr diffuses along the Cr grain boundaries (GBs) and locally oxidises when reacting with difussion O_2. The network grow when the discretized cells reach a connectivity threshold ϕ_c.
- t_2 **— Cr_2O_3 reduction and breakaway:** $3\,Zr + 2\,Cr_2O_3 \longrightarrow 4\,Cr + 3\,ZrO_2$, chromia reduction promotes voids formation through the oxide layer. The protection is lost completely when the void network reaches the surface.

7. Protection time and hydrogen production

Safety is governed by t_2, rather than by the oxide thickness. Between t_1 and t_2 the reduction consumes oxygen **already bound in the chromia**, resulting in internal oxygen re distribution without additonal H_2.

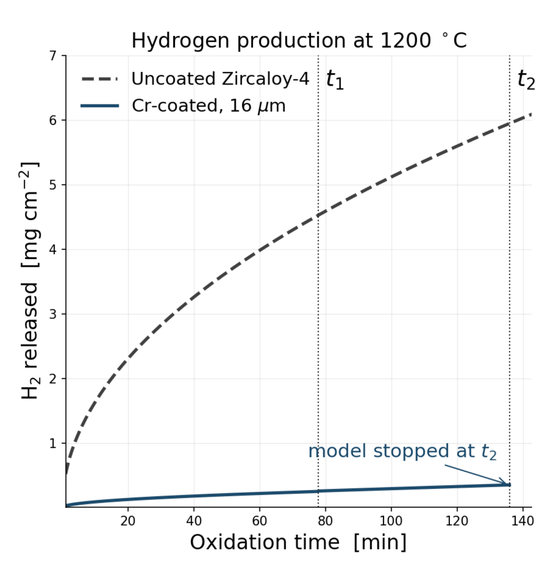

Figure 6: Simulated H_2 release for hypothetical coated and uncoated Zr alloy claddings.

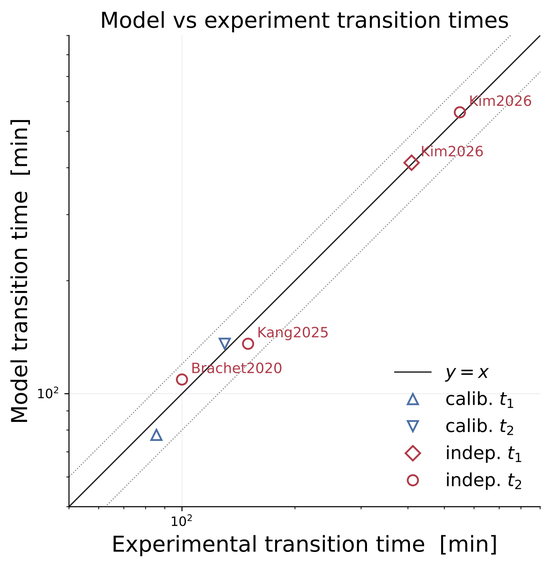

Figure 7: Transition times: model vs. exp. Blue markers: fitting cases; red markers: independent predictions.

H_2 production - Figure 6: Significant H_2 release is calculated for the ATF concept analyzed when compare to conventional Zr alloy.
Protection times - Figure 7: Both transition times are reproduced within $20\,\%$ of exp. values for different coating thickness and $1100\,^{\circ}C$ to $1300\,^{\circ}C$. A **single parameter** — Zr transport in the percolated network — is fitted at $1200\,^{\circ}C$. The resulting interval $t_2 - t_1$ of the independent datasets comes out within $6\,\%$ at 1100 and $1300\,^{\circ}C$.

Conclusions and outlook

- **Mechanistic simulation:** A five-phase ALE solver was developed that successfully captures coating degradation based on transport phenomena, obtaining safety margins ($t_2 - t_1$) within $6\,\%$ of available exp. data.
- **Safety impact:** The model accurately captures the mechanisms of the ATF potential benefits observed experimentally: delay massive H_2 production and coating degradation under SA conditions.
- **Future work:** Thermal transients implementation and bundle-scale extension.

References

[1] D. Kim, Y. Lee, Corros. Sci. **260** (2026) 113565. — [2] J.-C. Brachet *et al.*, Corros. Sci. **167** (2020) 108537. — [3] S. Wu *et al.*, J. Nucl. Mater. **589** (2024) 154836. — [4] D. Wang *et al.*, J. Nucl. Mater. **561** (2022) 153564. — [5] J. Yang *et al.*, J. Nucl. Mater. **547** (2021) 152806.